Int. J. Electrochem. Sci., 11 **(2016)** 7020 – 7030, doi: 10.20964/2016.08.42

International Journal of ELECTROCHEMICAL SCIENCE
www.electrochemsci.org

Structural and Electrochemical Properties of Electrodeposited Ni–P nanocomposite Coatings Containing Mixed Ceramic Oxide Particles

K. M. Zadeh, R. A. Shakoor[*]*, A. Bahgat Radwan*

Center for Advanced Materials (CAM), Qatar University (QU), Doha 2713, Qatar
[*]E-mail: shakoor@qu.edu.qa

Received: 8 May 2016 / *Accepted:* 11 June 2016 / *Published:* 7 July 2016

Mixed oxide ceramic particles were incorporated into Ni-P matrix to synthesize Ni-P-TiO_2-CeO_2 nanocomposite coatings. In the present study, the effect of concentration of mixed oxide ceramic particles (TiO_2 and CeO_2) on structural, surface and electrochemical properties of Ni-P coating is investigated. The coatings were electrodeposited on mild steel substrate and were then characterized using various techniques. The compositional (EDAX) confirms the co-deposition of TiO_2 and CeO_2ceramic particles into Ni-P matrix. The structural analysis (XRD) indicates that addition of mixed oxide ceramic particles do not have any prominent influence on the structure of Ni-P coatings as parent amorphous structure is preserved even at high concentration of mixed ceramic particles (7.5 g/l). The SEM and AFM analyses indicate that the synthesized coatings are of fine nodular morphology containing uniformly distributed ceramic particles. However, their excessive amount may lead to agglomeration and surface defects. The surface analysis (AFM) also indicates that the surface roughness increases with the increase in amount of TiO_2 and CeO_2 particles. The enhancement in roughness of coatings can be ascribed to the fact the added ceramic particles are hard and remain insoluble in the Ni-P matrix. The potentiodynamic polarization analysis confirms that incorporation of mixed oxide ceramic particles into Ni-P matrix improves its anticorrosion properties. However, their excessive amount may cause decrease in corrosion resistance due to formation of galvanic cells at the defective metal/coating interface.

Keywords: Coatings, composite, crystal structure, hardness, roughness, corrosion

1. INTRODUCTION

Electrodeposited Ni–P coatings on metal substrate have been widely used in many industries due to their superior properties [1-6]. The microstructure and properties of Ni–P coatings are

significantly influenced by the amount of phosphorus present in the coatings. For instance, Ni-P coatings with low phosphorus contents usually have a mixture of amorphous and microcrystalline microstructure with relatively high mechanical properties [7]. The properties of Ni-P coatings are also sensitive to the nature of the alloying elements and the second phase insoluble, hard ceramic particles used as reinforcing agents. In order to achieve desired properties, a careful selection of alloying additions and reinforcing agent is required. Improvement in corrosion resistance and mechanical properties has been achieved by the addition of ceramic reinforcing particles into Ni-P matrix by forming composite coatings. Different Ni-P composite coatings such as Ni–P–ZrO_2 [8] , Ni–P–TiO_2 [9], Ni-P-CeO_2 10], Ni-P-Si_3N_4 [11], Ni-P-Al_2O_3 [12] and Ni-P-SiC[13] have been developed on different substrate materials and their properties have been studied.

These metal oxide composite coatings have superior properties such as high hardness, high temperature oxidation resistance along with excellent wear and corrosion resistance. Abdel-Aal et al [14] studied nanostructured Ni–P–TiO_2 composite with different wt% of TiO_2. It is reported that Ni–P–TiO_2 nanocomposite coatings exhibit smaller grain size as compared with Ni–P coating 4.5 wt% of TiO_2. Another study undertaken by Prasanna et al [15] indicates that the amount of TiO_2 , reducing agent and plating parameters have considerable effect on the properties of synthesized coatings. They have noticed that the hardness of Ni-P coatings increases with increasing TiO_2 concentrations (4.5-10.0 wt. %). Yafeng Lian et al [16] studied the effect of cerium dioxide content on the friction and wear properties. It is found that the addition of CeO_2 can increase the micro hardness of the Ni-P coatings and the optimal adding amount of CeO_2 is ranging between 4 wt.% and 6 wt.%. However, study of Balaraju [17] et al on electroless Ni-P concludes that incorporation of second phase ceramic particles such as TiO_2, CeO_2 and Si_3N_4 to form Ni-P-TiO_2, Ni-P-CeO_2 and Ni-P-Si_3N_4 composite coatings does not have any influence on the structure and phase transformation behavior of electroless Ni–P coatings.

Never the less, incorporation of mixed reinforcing agent is getting substantial attention to alter the properties of Ni, Ni-P and Ni-B coatings. This is because of the reason that it is quite feasible and beneficial to get the desired set of properties by adding mixture of ceramic particles into the soft matrix having some specific and unique properties. A limited number of reports addressing the effect of mixed second phase particles on the properties of coatings have already been published indicating improvement in the properties of coatings [9, 18-20]. To the best of our knowledge, effect of addition of mixed TiO_2 and CeO_2 on the properties of Ni-P coatings has not been not reported so far. This will be the first report addressing the effect of incorporation of mixed oxides TiO_2 and CeO_2 particles on the properties of binary Ni-P coatings.

This research work reports the effect of concentration of mixed oxide ceramic particles on the Ni-P coatings developed through electrodeposition process. A comparative study on structural, surface and electrochemical properties of Ni-P and Ni-P-TiO_2-CeO_2 at various concentration of ceramic oxide particles has been under taken to elucidate the usefulness of addition of mixed oxide particles (TiO_2 and CeO_2) into Ni-P matrix. Owing to superior properties, the novel Ni-P-TiO_2-CeO_2 nanocomposite coatings may be well suited to many industrial applications.

2. EXPERIMENTAL

Ni-P, and Ni-P-TiO_2-CeO_2 nanocomposite coatings with varying amount of mixed nanoparticles (0, 2.5, 5.0 and 7.5 g/l) were synthesized using electrodeposition technique. The mild steel sheet was used as a substrate having size of 30 X 30 X1.5 mm.

2.1. Sample preparation

Prior to the coating process, the substrates were prepared using different SiC papers (180, 220, 320, 500, 800, 1000, 4000) leading to achieve flat and mirror like surfaces. After mechanical cleaning, all the substrates were further cleaned with acetone through sonication technique. The substrates were then thoroughly washed with distilled water and their surfaces were activated with 20 % solution of HCl for one minute. After activating the prepared surfaces, the substrates were thoroughly rinsed with distilled water and the electrodeposition process was started to develop coatings.

2.2. Coating baths preparation

The coating bath composition and operating conditions employed for the synthesis of Ni-P, and Ni-P-TiO_2-CeO_2 nanocomposite coatings through electrodeposition technique are presented in Table 1. We used nickel sulphate hexahydrate ($NiSO_4.6H_2O$) and nickel chloride hexahydrate ($NiCl_2.6H_2O$) as source of nickel, boric acid (H_3BO_3) as complexing agent, sodium hypophosphite (NaH_2PO_2) as source of phosphorous (P) and phosphoric acid as means to control the pH value of the coating baths. For coating synthesis, a nickel plate (99. 9%) and mild steel sheet (substrate) were used as anode and cathode respectively. It was assured that anode was placed parallel to the substrate in the plating bath. The Ni-P coatings were electrodeposited at 50 ±1˚C for a fixed deposition time of 30 minutes during which the coating bath was vigorously agitated with magnetic stirrer at 500 RPM using current density of 50 A/cm^2. The Ni-P-TiO_2-CeO_2 nanocomposite coatings containing concentration of mixed ceramic particles as 2.5 g/l were developed by adding TiO_2 (1.25 g/l) and CeO_2 (1.25 g/l) nanoparticles into a new and separately prepared Ni-P coating bath (Bath 1) keeping all the conditions similar as used for the synthesis of Ni-P coatings as mentioned above. Similarly, for the synthesis of Ni-P-TiO_2-CeO_2 nanocomposite coatings (5.0 g/l), another separate Ni-P coating bath (Bath 1) was prepared and TiO_2 (2.5 g/l) and CeO_2 (2.5 g/l) nanoparticles were added into the newly prepared coating bath. The coatings were then developed by employing the exact electrodeposition conditions as used for Ni-P and Ni-P-TiO_2-CeO_2 (2.5 g/l) nanocomposite coatings. Finally, TiO_2 (3.75 g/l) and CeO_2 (3.75 g/l) nanoparticles were added to a another separately prepared Ni-P coating bath (Bath 1) to synthesize Ni-P-TiO_2-CeO_2 (7.5 g/l) nanocomposite coatings employing the same procedure and electrodeposition conditions as mentioned above for other developed coatings.

Table 1. Coating baths and the operating conditions for the synthesis of Ni-P and Ni-P-TiO_2-CeO_2 nanocomposite coatings of various concentrations.

Number	Chemicals	Bath1 (Ni-P)	Bath 2 (Ni-P-TiO_2-CeO_2)
1	Nickle sulphate hexahydrate	250 g/l	250 g/l
2	Nickle chloride hexahytdrate	15 g/l	15 g/l
3	Boric acid	30 g/l	30 g/l
4	Phosphoric acid	6 g/l	6 g/l
5	Sodium hypophosphite	20 g/l	20 g/l
6	TiO_2 + CeO_2 particles	Nil	2.5, 5.0, 7.5 g/l
7	pH	2.3±1	2.3±1
8	Temperature	50 ±1˚C	50 ±1˚C
9	Deposition time	30 minutes	30 minutes
10	Bath agitation	500 RPM	500 RPM

2.3 Characterization

The chemical composition of the synthesized coatings was determined with Energy Dispersive X-Ray Spectroscopy (EDX) analysis. X-Ray diffractometer (XRD, Rigaku, Miniflex2 Desktop, Tokyo, Japan) equipped with Cu Kα radiations was used to determine phase purity and to conduct structural analysis. XRD patterns were recorded at room temperature in the 2Θ range of 20-80˚ at a scan speed of 1˚ min-1 with a step size of 0.01˚ applying 40 KV and 300 mA as voltage and current respectively. The coating morphology was studied using Field Emission Scanning Electron Microscope (FE-SEM, Nova Nano-450, and Netherland). The surface properties were studied using Atomic force microscopy (AFM, USA). Piezoelectric response AFM-3D (MFP-3D) Asylum research (USA) equipped with a Silicon probe (Al reflex coated Veeco model– OLTESPA, Olympus; spring constant: 2 N/m, resonant frequency: 70 kHz) was used in our experiments. All measurements were performed under ambient conditions using the Standard Topography AC air (tapping mode in air). An AFM head scanner applied with Si cantilever adjacent vertically in the sample resonant frequency of the free-oscillating cantilever set as the driving frequency.

The corrosion resistance of synthesized coatings in their as deposited states was evaluated by potentiodynamic polarization technique using Gamary 3000 (30K BOOSTER potentiostat/Galvanstate/ZRA, USA). All tests were performed at room temperature in 3.5 wt.% NaCl aqueous solution using a conventional three electrode cell consisting of a working electrode (substrate-mild steel sheet), saturated calomel reference electrode and a graphite counter electrodes. In all measurements the exposed area of the test sample was kept fixed to 0.785 cm^2. All the measurements were carried out at a scan rate of 0.167mV/sec.

3. RESULTS AND DISCUSSION

3.1. Co deposition of phosphorus and mixed oxide particles

The co-deposition of CeO_2 and TiO_2 ceramic particles into Ni-P matrix was confirmed with EDX analysis. The EDX results of Ni-P and Ni-P-TiO_2-CeO_2 nanocomposite coatings in their as

deposited state are presented in Figure 1. The presence of peaks of nickel (Ni) and phosphorus (P) in the EDX analysis of Ni-P coatings confirms the incorporation of (P) into nickel matrix. At the same time, the presence of additional peaks of titanium (Ti) and cerium (Ce) peaks in the in the EDX analysis also indicates the successful co-deposition of second phase oxide ceramic particles into Ni-P matrix.

3.2 Structural analysis

Figure 2 presents a comparison of XRD spectra of Ni-P and Ni-P-TiO_2-CeO_2 nanocomposite coatings containing at concentrations of CeO_2 and TiO_2 in their as deposited state. It can be noticed that Ni-P coating exhibits a single broad peak indicating amorphous structure of the deposited coatings. While increasing amount of TiO_2 and CeO_2 particles into Ni-P matrix does not alter the amorphous behavior of Ni-P coatings. This finding is consistent with the previous results [17]. However, the crystalline nature of added ceramic particles of TiO_2 and CeO_2 can be recognized in the XRD spectra.

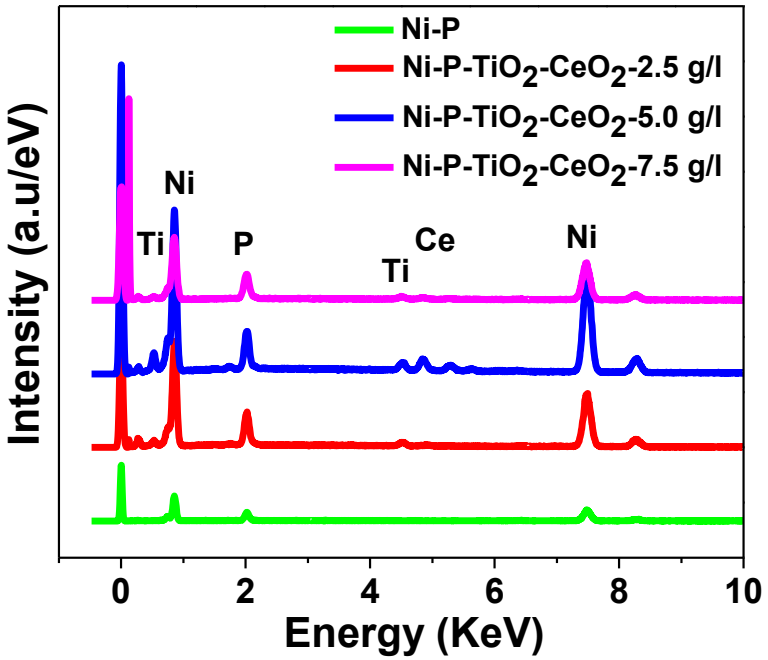

Figure 1. EDX analyses of Ni-P and Ni-P- TiO_2-CeO_2 coatings containing various concentration of mixed ceramic particles in their as deposited state.

3.3 Coating morphology

Figure 3 (a- d) shows the coating morphology of Ni-P and Ni-P-CeO_2-TiO_2 coatings containing different amount of mixed oxide particles. Ni-P and Ni-P-TiO_2-CeO_2 nanocomposite coatings are uniform and dense having nodular structure Fig. 3 (a-d). The presence of second phase particles can

be clearly seen (Figures 3 (b-d)) which is considered beneficial to improve the anticorrosion properties of coatings. These findings are consistent with the previous studies [9, 20]. At the same time, some agglomeration of mixed ceramic particles can also be noticed in the microstructure which leads to surface defects such as porosity.

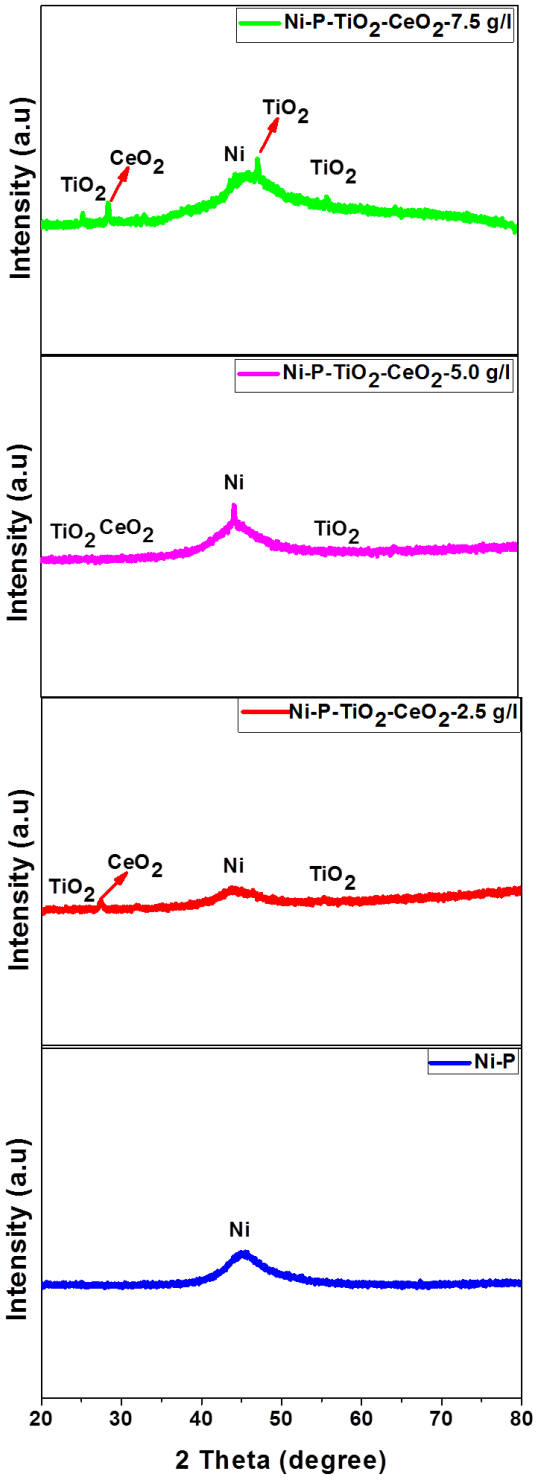

Figure 2. XRD analysis of synthesized coatings in their as deposited state at a scan speed of 1˚ min^{-1} with a step size of 0.01˚ at 40 KV and 300 mA.

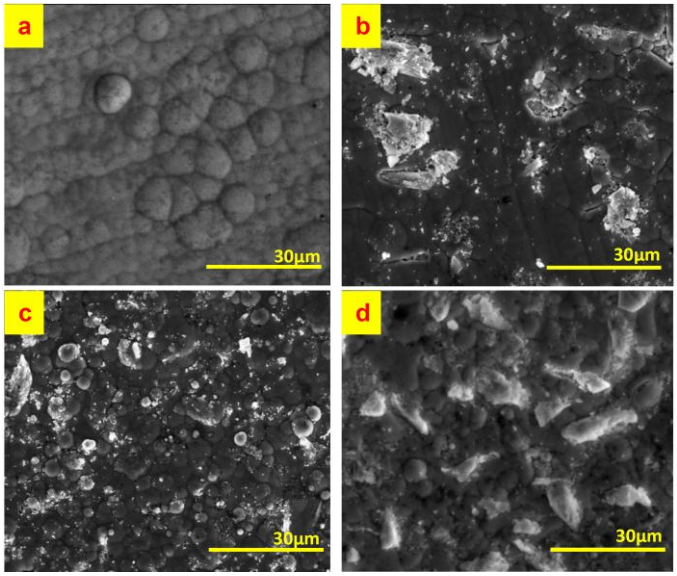

Figure 3. SEM analysis of synthesized coatings in their as deposited state (a) Ni-P (b Ni-P- TiO_2-CeO_2- 2.5 g/l (C) Ni-P- TiO_2-CeO_2-5.0 g/l (d) Ni-P-TiO_2-CeO_2 -7.5 g/l.

3.4 Surface analysis

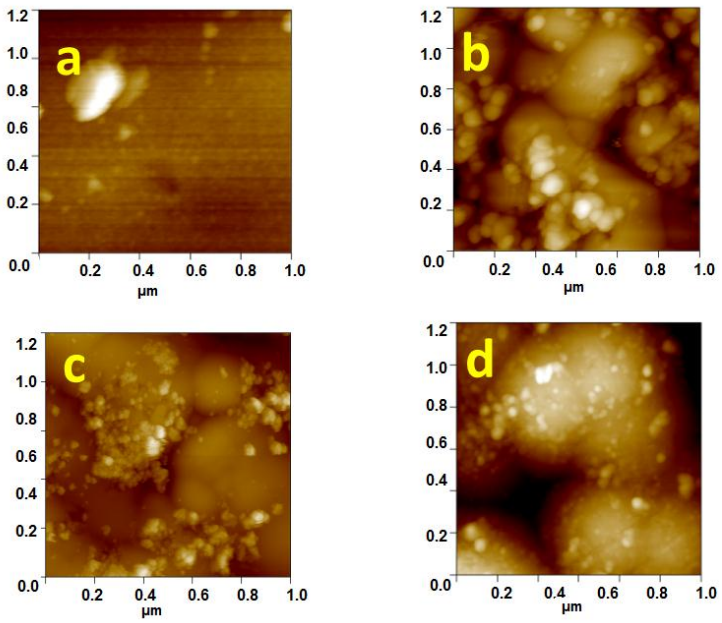

Figure 4. AFM images of synthesized coating sin their as deposited state (a) Ni-P (b Ni-P- TiO_2-CeO_2- 2.5 g/l (C)Ni-P- TiO_2-CeO_2- 5.0 g/l (d)Ni-P- TiO_2-CeO_2-7.5 g/l. Imaging was performed under ambient conditions using the Standard Topography in tapping mode in air.

In order to study the more details of coating morphology and surface properties, AFM analysis of the synthesized coating sin their as deposited state was under taken. A comparison of 3D images of Ni-P and Ni-P-TiO_2-CeO_2 coatings containing different concentration of mixed oxide particles is

shown in Figure 4. It can be noticed that coatings are uniform and dense having nodular morphology. The incorporation of second phase particles into the Ni-P matrix during the electrodeposition process can also be noticed. For a clear comparison, the surface roughness (R_a) values of the synthesized coatings were calculated from corresponding surface line profiles. The values of surface roughness of Ni-P, Ni-P-TiO_2-CeO_2 (2.5 g/l), Ni-P-TiO_2-CeO_2 (5.0 g/l) and Ni-P-TiO_2-CeO_2 (7.5 g/l) nanocomposite coatings are found to be 31 nm, 78 nm, 93 nm and 101 nm respectively. This observation confirms that the surface roughness increases with the increasing amount of second phase particles. This is due to the reason that mixed ceramic particles are hard and remain insoluble in the Ni-P matrix.

3.5. Corrosion behavior

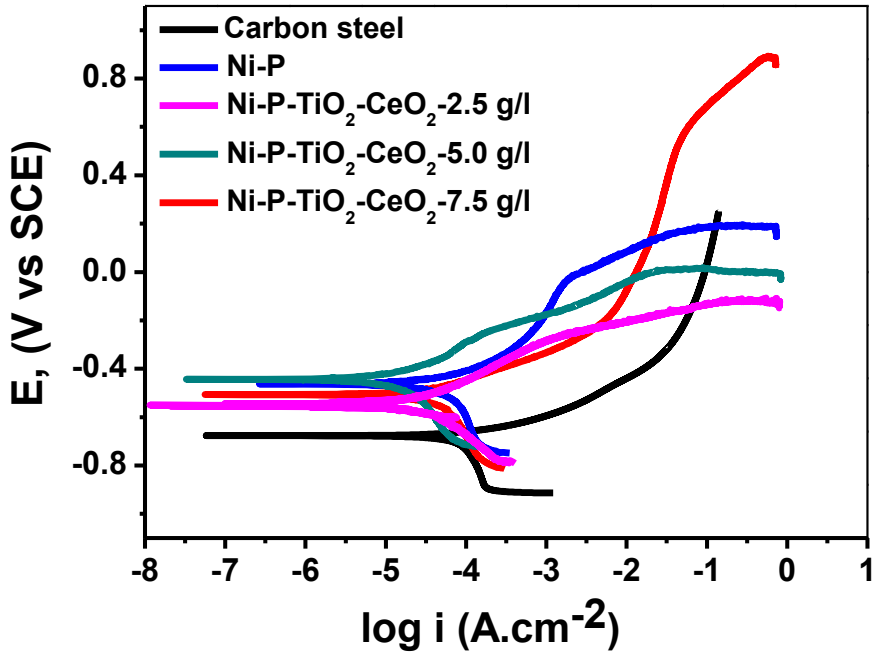

Figure 5. Tafel plots for uncoated Carbon steel substrate, Ni-P, Ni-P-TiO_2-CeO_2-2.5 g/l, Ni-P- TiO_2-CeO_2-5.0 g/l, Ni-P- TiO_2-CeO_2-7.5 g/l nanocomposite coatings after being tested in 3.5% NaCl aqueous solution at a scan rate of 0.167 mV s−1.

The corrosion behavior of electrodeposited Ni-P and Ni-P-TiO_2-CeO_2 nanocomposite coatings containing different concentration of mixed ceramic particles in 3.5 % NaCl aqueous solution was investigated at room temperature utilizing electrochemical method. Figure 5 displays the polarization curves for the carbon steel substrate, electroplated Ni–P and Ni-P-TiO_2-CeO_2 nanocomposite coatings containing different concentration of mixed ceramic particles. The cathode reaction in the polarization curves is related to the evolution of the hydrogen gas (H_2), while the anodic polarization curve is the most important features associated with the corrosion resistance.

The corrosion potential (E_{corr}), and corrosion current density (i_{corr}) of the carbon steel and electrodeposited coatings specimens were determined by extrapolating the linear sections of the anodic and cathodic Tafel lines. The corrosion protection efficiency (*PE*) of the synthesized coatings was calculated by applying the following relationship [21].

$$PE = 1 - \frac{i_2}{i_1} \times 100\%$$

Where i_1 and i_2 correspond to the corrosion current densities of the substrate and the coated samples, respectively. The corrosion potential (E_{corr}), anodic Tafel slope ($\mathcal{B}_a$), cathodic Tafel slope ($\mathcal{B}_c$) Corrosion current density (i_{corr}) and protection efficiency (*PE*) % of the carbon steel and coated samples obtained from polarization curves are listed in Table 2.

Table 2. Tafel analysis for uncoated Carbon steel substrate, Ni-P, Ni-P- TiO_2-CeO_2-2.5 g/l, Ni-P-TiO_2-CeO_2-5.0 g/l and Ni-P-TiO_2-CeO_2-7.5 g/l nanocomposite coatings after tested in 3.5% NaCl aqueous solution at a scan rate of 0.167 mV s−1.

Nomenclature	E_{corr} **(mV)**	i_{corr} **(μ A.cm^{-2})**	$\mathcal{B}_a$ **mv/decade**	$\mathcal{B}_c$ **mv/decade**	**Protection Efficiency (%)**
Carbon steel	678	86	284	365	--
Ni-P	466	50	189	278	41.8
Ni-P- TiO_2-CeO_2.2.5 g/l	555	33	166	244	61.6
Ni-P- TiO_2-$CeO_2$5.0 g/l	442	13	123	216	84.8
Ni-P- TiO_2-$CeO_2$7.5 g/l	504	46	135	228	46.5

The anodic and cathodic Tafel slope ($\mathcal{B}_a$,$\mathcal{B}_c$) decrease from 284 and 365 mv/decade for uncoated carbon steel to 123 and 216 mv/decade for Ni-P-TiO_2-CeO_2-7.5 g/l, indicating that the addition of mixed oxide nanoparticles (TiO_2 and CeO_2) hinder the chloride penetration to the metal surface and subsequently decrease the corrosion rate, see Table 2.

It can be noticed (Table 2) that electrodeposited Ni-P coating decreases the corrosion current density (i_{corr}) of carbon steel from 86 μA.cm^{-2} to 50 μA.cm^{-2}, which is attributed to the formation of amorphous structure of metallic coating. Kouwe et al. [22], ascribed the high corrosion resistance of Ni-P matrix to the adsorption of hypophosphite anions $(H_2PO_2)^-$ on the metal surface that hinders the penetration of H_2O species to the carbon steel. However Sankara et al [23], reported that the amorphous P in Ni-P matrix possess higher corrosion resistance than crystalline structure.

Addition of mixed oxides ceramic particles (2.5 g/l) decrease the i_{corr} and increase the (PE%) to 33 μA.cm^{-2} and 61.6%, respectively. Interestingly, the corrosion protection efficiency is reached to 84.8% when the concentration of mixed ceramic particles is increased to 5.0 g/l in the Ni-P coating. The combined effect of TiO_2-CeO_2 nanoparticles significantly enhanced the corrosion resistance of the

ceramic coatings in 3.5 wt.% NaCl. The process occurs by: (i) altering the microstructure, thereby stimulating the prevention of corrosion defect in the Ni-P matrix by acting as dielectric phase which lessen the adsorption of Cl^- ions onto the exposed area and (ii) uniform distribution of inert TiO_2 -CeO_2 in Ni–P alloy coating, resulting in formation of several corrosion microcells wherein CeO_2-TiO_2 ceramic particles and nickel metal act as cathode and anode, respectively. Therefore, more positive potential of TiO_2-CeO_2 than Ni^{+2} exist and subsequent occurrence of miscellaneous corrosion rather than localized corrosion takes place in Ni-P coating.

On the other hand, upon further increase in the concentration of mixed ceramic particles (7.5 g/l) the corrosion current density and protection efficiency decrease to 46 μAcm^{-2} and 46%, respectively. In this case, increasing the corrosion rate is attributed to the formation of defects in Ni-P coating such as pinholes and macro defects that act as active sites for initiation of pitting corrosion. Consequently, when the metallic coating is exposed to aggressive medium, nanocomposite coating will form galvanic cells at the defects of the metal/coating interface as the ceramic coatings are electrochemically more stable than the substrate (e.g. carbon steel). In addition, the XRD results indicates that the presence of high content of embedded nanoparticles influence the amorphous phase of Ni-P alloy which substantially decrease the corrosion resistance of Ni-P deposit [22].

4. CONCLUSIONS

Ni-P coatings incorporated with mixed oxide ceramic particles have been synthesized through electrodeposition process. The effect of concentration of mixed reinforcement on crystal structure, coating surface morphology and electrochemical properties has been investigated. It can be concluded that incorporation of mixed ceramic particles do not have significant influence on structural properties of Ni-P coatings. However, surface and anti-corrosion properties are highly dependent on the concentration of mixed ceramic particles. Noticeably, the surface roughness of Ni-P coatings increases with the increasing amount of mixed ceramic particles. Similarly, the corrosion resistance of Ni-P coatings increases with increasing amount of amount of mixed ceramic particles. However, their excessive amount causes agglomeration leading to surface defects which form galvanic cells at the defective metal/coating interface and thus reduces the corrosion resistance of the coatings.

References

1. W. Y. Chen, S. K .Tien, J. G Duh, *Surf. Coatings Technology.* 188 (2004) 489–494.
2. Z. Ping ,G. Cheng ,Y. He , *J. Mater. Sci. Tech.*. 26(2010) 945–950.
3. H. Jin, S. Jiang &L.N. Zhang , *Chinese Chem. Lett.* 19 (2008) 1367–1370.
4. L.Song, Y.Wang ,W. Lin, Q.Liu, *Surf. Coatings Technol.* 202 (2008)5146–5150.
5. D.H. Jeong, U. Erb, K.T. Aust, G.Palumbo, *Scr. Mater.* 48 (2003) 1067–1072.
6. J.N.Balaraju, N.Sankara & S.K.Seshadri, *J. Appl. Electrochem.* 33 (2003) 807–816 .
7. K.Keong, W. Sha, S.Malinov, *Surf. Coatings Tech.*. 168 (2003)263–274.
8. Y. Wang, R.A.Shakoor,R. Kahraman, *J. Alloys Compounds* 630 (2015)189–194 .
9. S.M.Shibli, V.S.Dilimon, *Int. J. Hydrogen Energy* 32 (2007) 1694–1700 .

10. H.Jin,S. Jiang& L.zhang, *J. Rare Earths* 27(2009) 109–113 .
11. T.Wang, G.Zhang, B. Jiang, *Appl. Surf. Sci.* 326 (2015) 162–167
12. S. Karthikeyan, B.Ramamoorthy, *Appl. Surf. Sci.* 307 (2014) 654–660
13. C.Ma, F. Wu,Y. Ning, F. Xia,Y. Liu, *Ceram. Int.* 40 (2014)9279–9284.
14. A.Abdel Aal, H. Hassan, M.Abdel Rahim, *J. Electrochem. Chem.* 619 (2008) 17–25.
15. P.Gadhari, P. Sahoo, *Procedia Engergy* 97 (2014) 439–448 .
16. Y.Lian, Q. Xue, *Wear* 181 (1995) 436–441.
17. J.Balaraju,T. Sankara,S. Seshadri, *Mater. Res. Bull.* 41(2006) 847–860.
18. K.H. Lee, D. Chang and S.C. Kwon, *Electrochim. Acta*., 50 (2005) 4538-4543.
19. T.V. Gaevskaya, I.G. Novotortseva and L.S. Tsybulskaya, *Metal Finishing*., 94 (1996) 100-103.
20. A. B. Radwan, R.A.Shakoor, A. Popelka, *Int. J. Electrochem. Sci*., 10 (2015) 7548-7562.
21. A. Budniok, A.Giewka, *J. Appl. Electrochem.* 27(1997) 1349–1354.
22. H.Luo, *Surf. Coat. Tech.* 277 (2015) 99–106.
23. V. Kouwe, *Electrochim. Acta* 38 (1993) 2093–2097

© 2016 The Authors. Published by ESG (www.electrochemsci.org). This article is an open access article distributed under the terms and conditions of the Creative Commons Attribution license (http://creativecommons.org/licenses/by/4.0/).